Olfactomedin 2: Expression in the Eye and Interaction with Other Olfactomedin Domain–Containing Proteins

Afia Sultana,[1] *Naoki Nakaya,*[1] *Vladimir V. Senatorov,*[1,2] *and Stanislav I. Tomarev*[1]

Purpose. Olfactomedin 2 (OLFM2) belongs to the family of olfactomedin domain–containing proteins. Genetic data suggest its association with glaucoma in Japanese patients. However, its functions are still elusive. In this study, the properties of mammalian OLFM2 were investigated.

Methods. Expression of the rat and mouse *Olfm2* gene was studied by using real-time PCR and in situ hybridization. Substitutions were introduced into OLFM2 by mutagenesis in vitro. Intracellular localization of OLFM2 was studied by confocal microscopy after transient transfection in HEK293 cells. Interaction of OLFM2 with olfactomedin 1 (Olfm1), olfactomedin 3 (Olfm3), myocilin, and gliomedin was studied by using co-immunoprecipitation.

Results. Two major human OLFM2 mRNAs encode secreted proteins with a length of 454 and 478 amino acids. OLFM2 is more closely related to OLFM1 and -3 than to any other family members. *Olfm2* showed the most dynamic expression pattern compared with *Olfm1* and *-3* during mouse eye development and was expressed preferentially in the developing retinal ganglion cell layer. Among three OLFM2 substitutions tested (T86M, R144Q, and L420S), only L420S completely blocked secretion of the protein. OLFM2 interacted with Olfm1 and -3, but not with myocilin and gliomedin. Co-transfection of the L420S mutant with wild-type Olfm1 and -3 significantly inhibited secretion of Olfm1 and -3.

Conclusions. Highly conserved OLFM2 protein may play an important role in the course of retinal and eye development. Severe mutations in one of the closely related olfactomedin domain–containing proteins (Olfm1–3) may block the secretion and probably the activity of all three family members, leading to more pronounced diseases of the retina than the knockout of individual genes. (*Invest Ophthalmol Vis Sci.* 2011;52:2584–2592) DOI:10.1167/iovs.10-6356

Olfactomedin was described almost 20 years ago as a novel 57-kDa glycoprotein exclusively expressed in the frog olfactory neuroepithelium.[1] Subsequent experiments by many laboratories demonstrated that olfactomedin contains a domain in its C terminus that is present in many proteins in species ranging from reef-building coral *Acropora millepora* (the phylum Cnidaria) to *Homo sapiens.*[2–7] This domain has a length of approximately 250 amino acids and was named the olfactomedin domain. There are at least 13 proteins containing the olfactomedin domain in mammals, and these proteins form a family.[4,8,9] This family segregates into seven subfamilies on the basis of domain organization, biochemical properties, and expression patterns.[4] The most studied olfactomedin domain–containing protein is myocilin. Mutations in the *Myocilin* gene are found in more than 10% of juvenile open-angle glaucoma cases and in 35% to 4% of patients with adult-onset primary open-angle glaucoma.[10–14] Myocilin proteins form subfamily III on a phylogenetic tree.[4,9] Three proteins, olfactomedin 1 (Olfm1), olfactomedin 2 (Olfm2), and olfactomedin 3 (Olfm3), form subfamily I. Olfm1 is also known as noelin in chicken and *Xenopus*,[15,16] pancortin in mice,[17] olfactomedin-related glycoprotein in rats,[18] and hOlfA in humans.[5] Olfm2 is also known as OlfC,[5] and Olfm3 is also known as optimedin.[19] These proteins are the most conserved among other olfactomedin domain–containing proteins.

High conservation of the amino acid sequences implies that Olfm1, -2, and -3 proteins have important functions. Indeed, overexpression of Olfm1 during embryonic development causes an excess of neural crest emigration in chicken,[15] leads to an expansion of the neural plate and enlargement of the neural tube and retina in *Xenopus*,[20] increases the thickness of the optic nerve and produces a more extended projection field in the optic tectum in zebrafish.[21] Inhibition of olfm1 expression by *olfm1*-specific morpholino oligonucleotides reduces eye size, inhibits optic nerve extension, and increases the number of apoptotic cells in the retinal ganglion cell and inner nuclear layers.[21] At the same time, elimination of the central (M region) part of Olfm1 in mice produces a relatively mild phenotype.[22] It has been shown that knockdown of olfm2 protein expression by morpholino oligonucleotides produces a phenotype that is very similar to that described for the olfm1 knockdown in zebrafish.[23] Genetic data indicate that mutation of the *OLFM2* gene in humans leading to the R144Q substitution in the protein sequence is a possible disease-causing mutation in Japanese patients with open-angle glaucoma.[24] The T86M substitution in the OLFM2 protein has been associated with colorectal cancers.[25] Overexpression of Olfm3 inhibits neurite outgrowth and induces Ca^{2+}-dependent aggregation of NGF-stimulated PC12 cells.[26] It has been suggested that the expression of Olfm3 stimulates the formation of adherens and tight junctions and modulates cytoskeletal organization, cell–cell adhesion, and cell migration in the brain and retina.[26]

In this study, we investigated the properties of mammalian OLFM2. *Olfm2* and *-1* showed an overlapping expression pattern in the course of eye development in the rat. OLFM2 interacted with Olfm1 and -3 but not with the more distantly related proteins myocilin and gliomedin. Although the R144Q and T86M substitutions did not inhibit secretion of OLFM2, L420S substitution in the olfactomedin domain of OLFM2, which corresponds to the I477S mutation in human myocilin,

From the [1]Section of Molecular Mechanisms of Glaucoma, Laboratory of Molecular and Developmental Biology, National Eye Institute (NIH), National Institutes of Health, Bethesda, Maryland.

[2]Present affiliation: New York Medical College, New York, New York.

Supported by the Intramural Research Program of the National Eye Institute, National Institutes of Health.

Submitted for publication August 6, 2010; revised November 10, 2010; accepted November 16, 2010.

Disclosure: **A. Sultana**, None; **N. Nakaya**, None; **V.V. Senatorov**, None; **S.I. Tomarev**, None

Corresponding author: Stanislav I. Tomarev, Molecular Mechanisms of Glaucoma Section, Laboratory of Molecular and Developmental Biology, National Eye Institute, NIH, 5635 Fishers Lane, Room 1124, Bethesda, MD 20892-9303; tomarevs@nei.nih.gov.

inhibited its secretion. Moreover, secretion of wild-type Olfm1 or -3, but not myocilin, was inhibited in the presence of this mutation. We suggest that severe mutations in one of the closely related olfactomedin domain–containing proteins (Olfm1-3) blocks secretion and probably activity of the whole subfamily.

METHODS

Characterization of Olfm2 Isoforms and Their Comparison with Other Family Members

Human and mouse *OLFM2* mRNA sequences (NM_058164.2 and NM_173777.3) were used as queries to search human and mouse EST databases with BLAST, using the NCBI (National Center for Biotechnology Information) server to identify the EST sequences that have homology to the query. A pair-wise BLAST search was performed for the genomic and EST sequences differing at the N- and C termini. Location and size of introns and exons were determined by comparing the coordinates of query and subject and by ensuring the presence of putative splice junctions. The AceView gene database (www.ncbi.nlm.nih.gov/IEB/Research/Acembly; provided in the public domain by the NCBI, Bethesda, MD) was also searched for human and mouse *OLFM2* isoforms.[27] Protein information resource (PIR; http://pir.georgetown.edu/ provided in the public domain by Georgetown University, Washington, DC, and the University of Delaware, Newark, DE) was used to build multiple sequence alignments and to identify percent identities between OLFM2 and other family members. The Exon-Intron Graphic Maker (http://wormweb.org/exonintron/ developed by Nikhil Bhatla and provided in the public domain by Massachusetts Institute of Technology, Cambridge, MA) was used to draw the structure of the human and mouse *OLFM2* genes and their isoforms. SignalPV2.0 (http://www.cbs.dtu.dk/services/SignalP-2.0/ provided in the public domain by the Center for Biological Sequence Analysis, Technical University of Denmark, Lyngby, Denmark) and PSORTII (Prediction of Protein Sorting Signals and Localization Sties in Amino Acid Sequences; http://psort.nibb.ac.jp/ developed by Kenta Nakai, and provided in the public domain by the University of Tokyo, Tokyo, Japan) was used to predict the signaling peptides in OLFM2 isoforms and its cellular localization.

Quantitative PCR and In Situ RNA Hybridization

All the animals used in the experiments were managed according to the ARVO Statement for the Use of Animals in Ophthalmic and Vision Research. RNA was isolated from mouse eyes and brain at developmental or postnatal stages indicated later (RNAzol; TelTest, Friendswood, TX). Total mouse heads (without eyes) instead of brain were used to isolate RNA at postconception days (dpc) 13.5 and 16.5. Two micrograms of isolated total RNA was used as a template to synthesize cDNA (cDNA Reverse Transcription Kit; Applied Biosystems, Inc. [ABI], Rockville, MD). cDNA was used as a template for quantitative PCR reactions using a SYBR Green PCR master mix (ABI) and a real-time thermocycler (7900HT; ABI). Each sample was analyzed in triplicate (technical replicates). The ratios of change in the expression levels were calculated by using the Ct values. Transcript abundance was normalized to the adult stage. Primers for the *Olfm1*, *-2*, and *-3* (*Olfm 1-3*) genes were designed for the regions that were common for all isoforms. Expression of *Olfm1-3* in the adult eye and brain was analyzed with two different sets of primers for each gene, using two independent RNA samples (biological replicates). Student's *t*-test was used to measure statistical significance. The following primers were used: *Olfm1-a* forward 5′-GGAGAAGATGGAGAACCAGATGA-3′ and *Olfm1-a* reverse 3′-TGCCTGGCTAGATGCTGCTT-5′; *Olfm1-b* forward 5′-GGGATAGTGAGGGCAGGTGT-3′ and *Olfm1-b* reverse 3′-CGGGCTATGGATTGAGACAT-5′; *Olfm2-a* forward 5′-GACACAATGGCCCCCAGT-3′ and *Olfm2-a* reverse 3′-ACGGAACTCCAGCACTCG-5′; *Olfm2-b* forward 5′-GTATGTTCGCAGCATGGAGA-3′ and *Olfm2-b* reverse 3′-CAATGGTTCGTGTGTCTGCT-5′; *Olfm3-a* forward 5′-GCTTCGCCAGCTACTGGAAAA-3′ and *Olfm3-a* reverse 3′-ATCTGCCGAAACTTGGCCTTC-5′; and *Olfm3-b* forward 5′-GAAGGCCAAGTTTCGGCAGAT-3′ and *Olfm3-b* reverse 3′-GGCAGTAGCTCATCCATTTTCT-5′.

For in situ hybridization, rat embryos at dpc 12, 15, and 18 were fixed in 4% paraformaldehyde in 0.1 M phosphate-buffered saline (PBS; pH 7.4) overnight and processed for paraffin embedding. Serial sections (6 μm) were hybridized with specific ^{33}P-labeled riboprobes. To prepare the riboprobes, PCR fragments of rat *Olfm1* (accession number NM_053573, position 2064-2605) and *Olfm2* (accession number XM_233742, position 122–625) cDNAs were cloned into a vector (pCRII-TOPO; Invitrogen, Carlsbad, CA). Plasmids were linearized, and antisense probes were transcribed from the T7 promoter. In situ hybridization, washes, and autoradiography were performed as previously described.[28]

DNA Constructs for *OLFM2*

The human full-length *OLFM2* cDNA (454 amino acids) cloned into the pCMV6 vector containing the C-terminal tag (hOLFM2-FLAG) was purchased from OriGene (Rockville, MD). Human OLFM2 construct containing the N-terminal FLAG tag (FLAG-hOLFM2) was generated by placing 2× FLAG sequences in a reading frame after the signaling peptide in hOLFM2 and cloning into the pcDNA3.1 vector. Two amplification steps were used to make this construct. Oligonucleotides (hOLFM2–1F) 5′-AAGCTTATGTGGCCGCTCACGGTCCCGCCG-3′ and (hOLFM2–1R) 3′-GGATCCCTTATCGTCGTCATCCTTGTAATCCTTATCGTCGTCATCC TTGTAATCTGGGTTCTGGAAGAGAGTCTG-5′ were used for the first step, and oligonucleotides (hOLFM2–2F) 5′GGATCCCAGACTCTCTTCCAGAACCCA-3′ and (hOLFM2–2R) 3′-GAATTCTCAGGGGTCCCCAGAGGTGCT-5′ were used for the second step. Purified fragments were digested with *Hin*dIII, *Bam*HI, and *Bam*HI, *Eco*RI, respectively, and ligated into the pcDNA3.1 vector. Human OLFM2 construct (hOLFM2) without any tag was generated by amplifying the coding region of hOLFM2 from OriGene cDNA, with oligonucleotides hOLFM2–1F 5′-AAGCTTATGTGGCCGCTCACGGTCCCGCCG-3′ and hOLFM2–2R 5′-GAATTCTCAGGGGTCCCCAGAGGTGCT-3′. A purified PCR fragment was digested with *Hin*dIII and *Eco*RI and cloned into the pcDNA3.1 vector.

Production of hOLFM2 Mutants

The *FLAG-hOLFM2* construct was used as a template for generating the T86M, R144Q, and L420S mutants. All constructs were generated by site-directed mutagenesis (QuickChange; Stratagene, La Jolla, CA). The following primer pairs were used: T86MF: 5′-CCTTGAGTTGCGATGTATCGCGACCTCC-3′ and T86MR: 3′-GGAACTCAACGCCTACATAGCGCTGGAGG-5′; R144QF: 5′-TACAAGGCAGACACGCAGACCATTGTACGCTTG-3′ and R144QR: 3′-ATGTTCCGTCTGTGCGTCTGGTAACATGCGAAC-5′; and L420SF: 5′-ATTCCCACATCTCGATGTCGGATTACAACCCCCGGG-3′ and L420SR: 5′-CCCGGGGGTTGTAATCCGACATCGAGATGTGGGAAT-3′. The identity of all constructs was confirmed by sequencing.

Cell Culture, Transfection, Deglycosylation, and Western Blot Analysis of hOLFM2

HEK293, NIH3T3, and COS7 cells were cultured in Dulbecco's modified Eagle's medium (DMEM) supplemented with 10% fetal bovine serum (FBS) in 5% CO_2 at 37°C. The cells were transiently transfected with corresponding plasmids with lipophilic transfection reagent (Lipofectamine 2000; Invitrogen, Carlsbad, CA). Serum-containing medium was replaced 12 hours after transfection with serum-free medium and the cells were incubated for an additional 48 hours After that, conditioned medium (CM) was collected, and the cells were lysed in lysis buffer (10 mM Tris [pH 7.5], 5 mM EDTA, 0.15 M NaCl, 1% Triton X-100, 1 mM DTT, 5 mM NaF, 0.5 mM Na_3VO_4, 10% glycerol, and protease inhibitor cocktail; Roche, Indianapolis, IN). Proteins were separated by SDS-PAGE followed by Western blot analysis with the FLAG monoclonal antibody (Sigma-Aldrich, St. Louis, MO). For deglycosylation, CM and lysates of transiently transfected HEK293 cells were predenatured in the glycoprotein denaturing buffer (0.5% SDS and 40

mM DTT) at 100°C for 10 minutes. Denatured proteins were treated with 5000 units of PNGase F (500 U/μL; Sigma-Aldrich) at 37°C for 16 hours, followed by SDS-PAGE and Western blot analysis with the FLAG monoclonal antibody. A chemiluminescence system (SuperSignal West Dura; Pierce, Rockford, IL) was used for detection.

Immunofluorescence

For the study of the intracellular distribution of OLFM2, HEK293 cells were plated on chambered slides (Laboratory-Tek; Nulge Nunc Internaternational, Naperville, IL) and transfected with the *FLAG-OLFM2* construct (Clontech, Mountain View, CA). Twenty-four hours after transfection, the cells were fixed in 4% paraformaldehyde in PBS (pH 7.4) for 10 minutes, washed three times in PBS, and permeabilized with 0.1% Triton X-100 in PBS for 5 minutes. After the cells were washed three times with PBS, they were blocked with 2% bovine serum albumin (BSA) for 30 to 60 minutes and incubated with the monoclonal mouse anti-FLAG (dilution 1:2000) and rabbit anti-calnexin (1:50; Cell Signaling Technology, MA) antibodies overnight at 4°C. The cells were then washed with PBS two to three times and visualized with AlexaFluor 488 mouse and AlexaFluor 594 rabbit antibodies at 1:400 dilution (Invitrogen-Molecular Probes, Eugene, OR).

Polyclonal Antibody Production

Olfm2 polyclonal peptide antibody was produced against the peptide RSLDARLRAADGSVSAKSF corresponding to amino acids 101 to 119 of human OLFM2 (Fig. 2), using the custom immunology services of Covance Research Company (Princeton, NJ). The specificity of the antibody was checked using the lysates from HEK293 cells and HEK293 cells transfected with Olfm1, myocilin, or OLFM2.

Co-immunoprecipitation

HEK293 cells were transiently co-transfected with 4 μg of *FLAG-hOLFM2* and optimedin–*Myc*[19]; *Olfm1*, or gliomedin ectodomain-His,[29]; or *OLFM2* and *FLAG-Myocilin*[30] expression constructs (Lipofectamine 2000; Invitrogen). Serum-containing medium was replaced 12 hours after transfection with serum-free medium. After an additional 36 hours, the serum-free medium was collected, and the cells were washed with PBS twice and lysed in lysis buffer (50 mM Tris [pH 7.5], 150 mM NaCl, 1% NP-40, 5% glycerol, and protease inhibitor cocktail; Roche, Indianapolis, IN) for 15 minutes on ice followed by centrifugation at 12,000*g* for 10 minutes. Cleared CM and culture lysates (CLs) were immunoprecipitated with anti-FLAG M2 beads overnight at 4°C. After incubation, the beads were washed three times in lysis buffer. Immunoprecipitates were analyzed by Western blot analysis with Myc, Olfm1, and Olfm2 antibodies. For reverse immunoprecipitation between OLFM2 and Olfm3, cleared CM and CLs were incubated with Myc monoclonal antibody (Cell Signaling Technology) for 1 hour at 4°C. After incubation with the antibody, protein-G agarose beads were added to the samples and incubated overnight at 4°C. After the beads were washed three times with lysis buffer, the immunoprecipitates were analyzed by Western blot analysis using Olfm2 and Myc polyclonal antibodies. Reverse IP between OLFM2 (without any tag) and FLAG-Olfm1 was performed with anti-FLAG M2 beads using the same method. Immunoprecipitates were analyzed by Western blot analysis, with Olfm1 and Olfm2 antibodies.

Results

Olfm2 Structure and Its Similarity with Other Family Members

The *OLFM2* gene is located on chromosome 19, region p13.2, in humans. It spans almost 83 kbp and consists of eight exons. Two major mRNAs encode proteins with a length of 454 and 478 amino acids (Figs. 1A, 2). These two proteins are identical with the exception of the N-terminal sequences encoded by different exons transcribed from different promoters. mRNA encoding the longer form was preferentially identified in retinoblastoma, whereas mRNA encoding the shorter form was found mainly in the neuronal tissues (ESTs). Both major forms contain potential signaling peptides predicted by different algorithms (Fig. 2). According to the PSORT prediction program, the probabilities of OLFM2 (454 amino acids) localization in the extracellular region, the endoplasmic reticulum, cytoplasm, and mitochondria are 66.7%, 11.1%, 11.1%, and 11.1%, respectively. One cDNA clone encoding an OLFM2 form with a length of 376 amino acids has been identified in thymus (ESTs). This mRNA is transcribed from a different promoter and contains an untranslated first exon (Fig. 1A, exon 4). This minor form does not have a signaling peptide. The methionine, which is internal in the two major forms (Fig. 2, position 79), is used as the initiator methionine in 376 amino acid form. The N-terminal parts of the longer OLFM2 forms contain two coiled–coiled regions that may be involved in dimer formation, whereas the C-terminal part of all forms encoded by exons 7 and 8 contains the olfactomedin domain.

The rodent *Olfm2* gene has a similar organization as the human *OLFM2* gene with few exceptions. Three mouse *Olfm2* forms transcribed from different promoters have been identified. They encode 448, 456, and 478 amino-acid-long proteins (Fig. 1B, Fig. 2). The last two forms are orthologous to the major human OLFM2 forms.

In humans, OLFM2 shares the highest identity with OLFM1 and -3 (60% and 61%, respectively). Its identity with myocilin is 31%. However, when only the olfactomedin domains of these proteins are compared, the identity between OLFM2 and OLFM3, OLFM1, and myocilin are increased to 66%, 65%, and 40%, respectively. OLFM2 is a highly conserved protein. The human OLFM2 protein shows 98%, 81%, and 78% identity with the mouse, *Xenopus*, and zebrafish Olfm2 proteins, respectively (Fig. 2).

Expression Pattern of *Olfm2* in Mammals

Expression of the *Olfm2* gene has been previously investigated in zebrafish.[31] In zebrafish, *Olfm2*, similar to *Olfm1a* and *-1b* genes, is preferentially expressed in the developing central

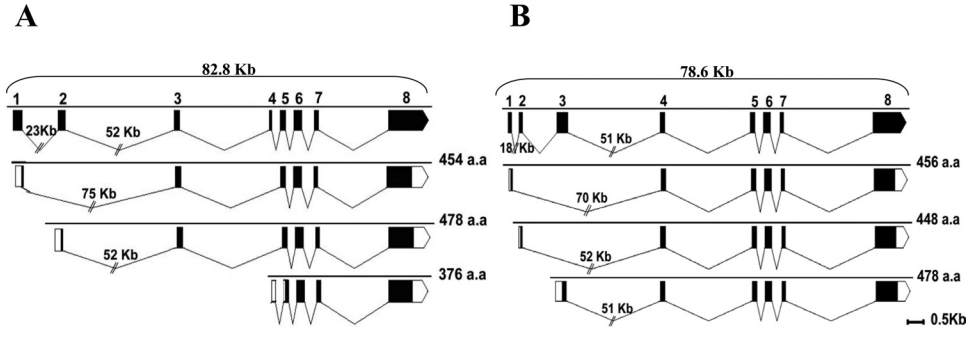

Figure 1. Structural characterization of the *OLFM2* gene. The exon–intron structure of the human (**A**) and mouse (**B**) *OLFM2* genes. The diagram in (**A**) and (**B**) shows human and mouse *OLFM2* genes drawn approximately to scale with the exception of introns 1 and 2 in the human gene and introns 1 and 3 in the mouse gene. The three alternatively spliced mRNAs are shown.

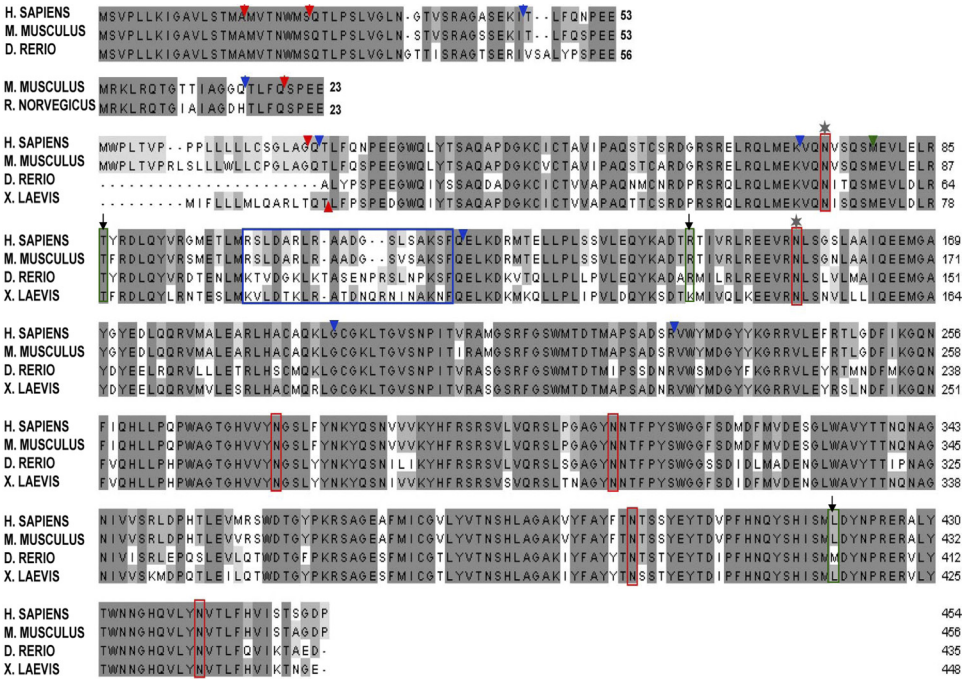

FIGURE 2. Comparison of the major human OLFM2 sequence with those of other species. Different N-terminal sequences encoded by different exons and found in identified OLFM2 isoforms are shown at the *top*. *Blue triangles*: positions of introns; *red triangles*: potential cleavage sites; *green triangle*: the initiator methionine in the minor human OLFM2 form with a length of 376 amino acids; *blue box*: the amino acids against which the peptide antibody is synthesized; *red boxes*: potential glycosylation sites. *Two experimentally confirmed glycosylation sites.[32] (↓) The position of mutations (T86M, R144Q, and L420S) that were used in this work.

nervous system, as well as in neural-crest–derived structures.[23,31] Here, we studied the expression pattern of the *Olfm2* gene in mammalian brain and eye and compared it with the expression patterns of the *Olfm1* and *-3* genes. *Olfm2* showed the most dynamic pattern of expression compared with *Olfm1* and *-3* in the course of mouse eye and brain development, as judged by real-time PCR (Figs. 3A, 3B). The primers that we used amplify all forms of *Olfm1*, *-2*, or *-3*. Expression of *Olfm2* changed significantly during embryonic eye development with the maximum level of expression detected around 19.5 dpc. *Olfm2* was downregulated postnatally. *Olfm1* showed a similar time course of expression with smaller variations between maximum and minimum values, whereas *Olfm3* showed a practically constant level of expression in the eye between 13.5 dpc and adulthood (Fig. 3A). In the brain (total heads without eyes were used for 13.5 and 16.5 dpc), the level of *Olfm2* expression increased from 13.5 dpc to early postnatal age (postnatal day 6 was analyzed) and decreased in the adult brain (Fig. 3B). The levels of *Olfm1* and *-3* mRNAs increased moderately in the course of embryonic development and remained stable in the postnatal brain (Fig. 3B). The relative abundance of Olfm1–3 mRNAs was examined by real-time PCR with two independent pairs of primers for each gene (see the Materials and Methods section). For each gene, the Ct values obtained with two independent pairs of primers were very similar. Therefore, we concluded that the Ct values reflect the relative abundance of corresponding transcripts. The levels of *Olfm1* mRNA in adult eye and brain were higher than the levels of *Olfm2* and *-3* mRNAs (Figs. 3C, 3D). The levels of *Olfm1* mRNA were also higher than the levels of *Olfm2* and *-3* mRNAs during the developmental stages analyzed, whereas the levels of *Olfm2* mRNA were higher than the levels of *Olfm3*

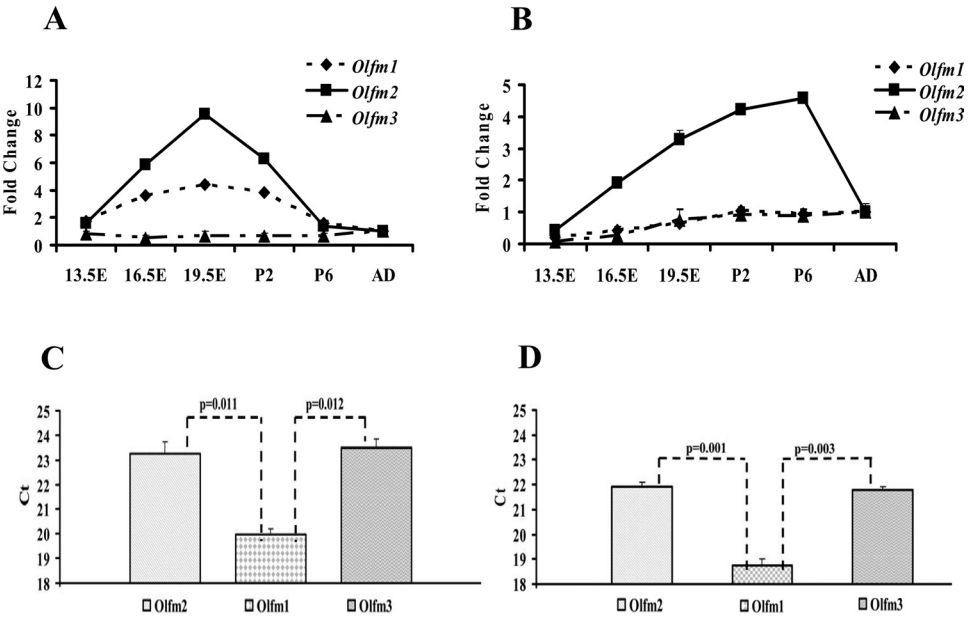

FIGURE 3. Changes in the levels of mRNAs encoding *Olfm1*, *-2*, and *-3* in the mouse eye (**A**) and brain (**B**) as judged by real-time PCR. Total heads without eyes were used for brain RNA isolation from 13.5 dpc (13.5E) and 16.5 dpc (16.5E) embryos. The levels of mRNA were calculated relative to their levels in adult tissues for each gene. Normalization was performed using *GAPDH* mRNA. Relative abundance of *Olfm1-3* mRNAs was evaluated on the basis of Ct values for *Olfm1*, *-2*, and *-3* mRNAs in the adult eye (**C**) and brain (**D**). AD, adult.

mRNA during development and early postnatal development in the analyzed tissues (data not shown).

Expression patterns of *Olfm1-3* were also studied by in situ hybridization. In the eye, expression of *Olfm2* preceded *Olfm1* expression and was first detected 12 dpc in the developing neural retina and retinal pigmented epithelium (Fig. 4). At this developmental stage, expression of *Olfm1* was not detected in the eye. *Olfm1* and *-2* were preferentially expressed in the differentiating retinal ganglion cells between 15 and 18 dpc (Fig. 4). Similar to PCR results, *Olfm1* showed a stronger hybridization signal than *Olfm2* with the probes used. The *Olfm3* in situ probe showed even weaker hybridization signals than the *Olfm2* probe in the developing rat eye, which prevented unambiguous identification of the expression sites (not shown).

OLFM2 Is a Secreted Glycosylated Protein

Since the major forms of OLFM2, similar to OLFM1 and -3, contain a signaling peptide, we checked whether OLFM2 is secreted from mammalian cells. HEK293 cells were transfected with a cDNA construct encoding the main human OLFM2 (454 amino acid form) in frame with the FLAG tag at the C terminus (OLFM2-FLAG) or at the N terminus immediately after the signaling peptide (FLAG-OLFM2). The CL and CM were first analyzed by Western blot analysis with the FLAG monoclonal antibody 48 hours after transfection. OLFM2-FLAG and FLAG-OLFM2 were detected in cell lysates (Figs. 5A, 5B), whereas only FLAG-OLFM2, not OLFM2-FLAG, was detected in CM (Figs. 5A, 5B) as a band with apparent molecular mass of more than 60 kDa when detected with the FLAG antibody. Olfm2 peptide antibody detected secretion of OLFM2 in CM with the OLFM2-FLAG construct; however, the secretion was significantly less efficient than the FLAG-OLFM2 construct (Fig. 5C). Since the OLFM2-FLAG construct was not secreted efficiently, we did not use this construct in subsequent experiments. Similar to FLAG-OLFM2, OLFM2 without any tag was detected both in cell lysate and CM with Olfm2 peptide antibody (Fig. 5C). In general, secretion of FLAG-OLFM2 was not as efficient as secretion of other family members, such as OLFM1, OLFM3, and myocilin. Since the predicted molecular mass of OLFM2 is 51 kDa, the higher apparent molecular mass of the detected protein suggests that OLFM2 is glycosylated. Indeed, several potential glycosylation sites (positions 74, 155, 275, 310, 399, and 441 in the human 454-amino-acid OLFM2 form and positions 76, 157, 277, 312, 401, and 443 in the mouse 456-amino-acid Olfm2 form; Fig. 2) were predicted by using the PROSITE program (http://expasy.org/prosite; provided in the public domain by the Swiss Institute of Bioinformatics, Geneva, Switzerland). N-glycosylation at positions 76 and 157 of the mouse sequence has been recently demonstrated experimentally.[32] The glycosylation sites in Olfm2 proteins from different species are completely conserved (Fig. 2), suggesting the importance of these sites for biological activity of OLFM2. Treatment of CLs and CM with the deglycosylating enzyme PNGase F reduced the size of the detected protein to approximately 51 kDa, demonstrating that OLFM2 is a glycoprotein (Fig. 5D).

Intracellular localization of OLFM2 was studied after transfection of HEK293 cells with FLAG-OLFM2. Immunostaining of these cells with antibodies against the FLAG epitope and calnexin indicated that FLAG-OLFM2 co-localized with the endoplasmic reticulum marker in the perinuclear region (Fig. 5E).

OLFM2 Interacts with Some Other Family Members

It has been well demonstrated that Olfm1, Olfm3, and myocilin are able to form homodimers and that the N terminus of these proteins is essential for dimerization.[19] We tested whether OLFM2 is able to form heterodimers with other family members. HEK293 cells were co-transfected with FLAG-OLFM2 and Olfm1, Olfm3-Myc, or gliomedin ectodomain-His, or with OLFM2 and FLAG-myocilin constructs. CM and cell lysates were immunoprecipitated with FLAG beads 48 hours after transfection, and the immunoprecipitates were analyzed by Western blot analysis with corresponding antibodies. The re-

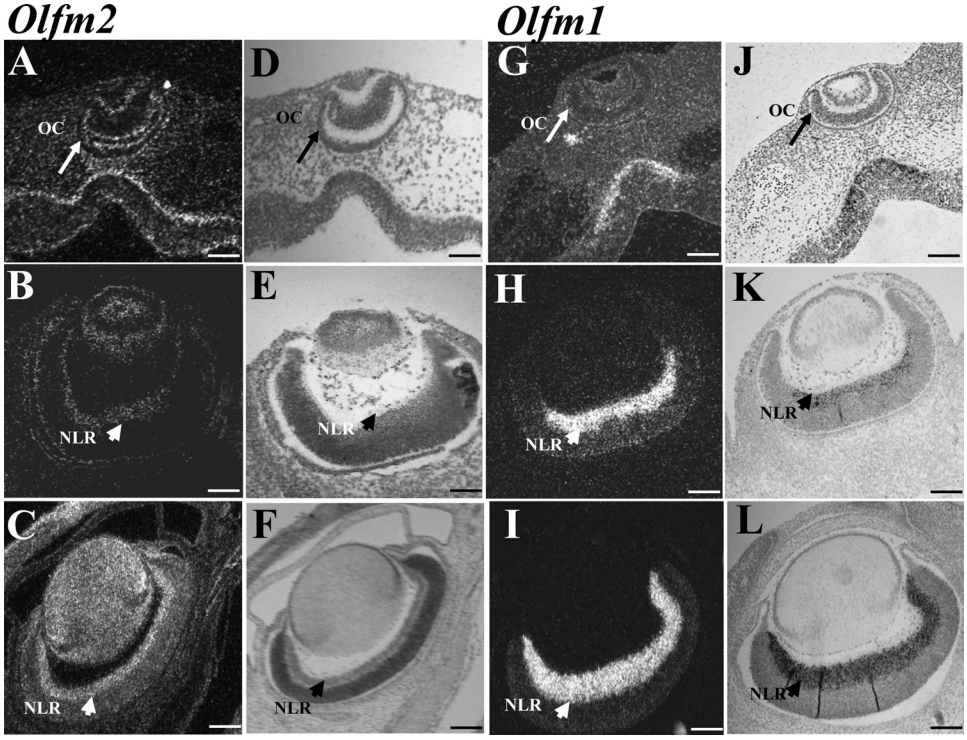

FIGURE 4. Radioactive in situ hybridization of *Olfm2* (**A–C** dark field; **D–F** bright field) and *Olfm1* (**G–I** dark field; **J–L** bright field) antisense probes with embryonic rat eye sections. Localization of mRNAs was analyzed at 12 (**A**, **B**), 15 (**C**, **D**), and 18 (**E**, **F**) dpc. *Arrows*: optic cup (OC); *arrowheads*: differentiating retinal ganglion cell layer (NLR). Scale bar, 100 μm.

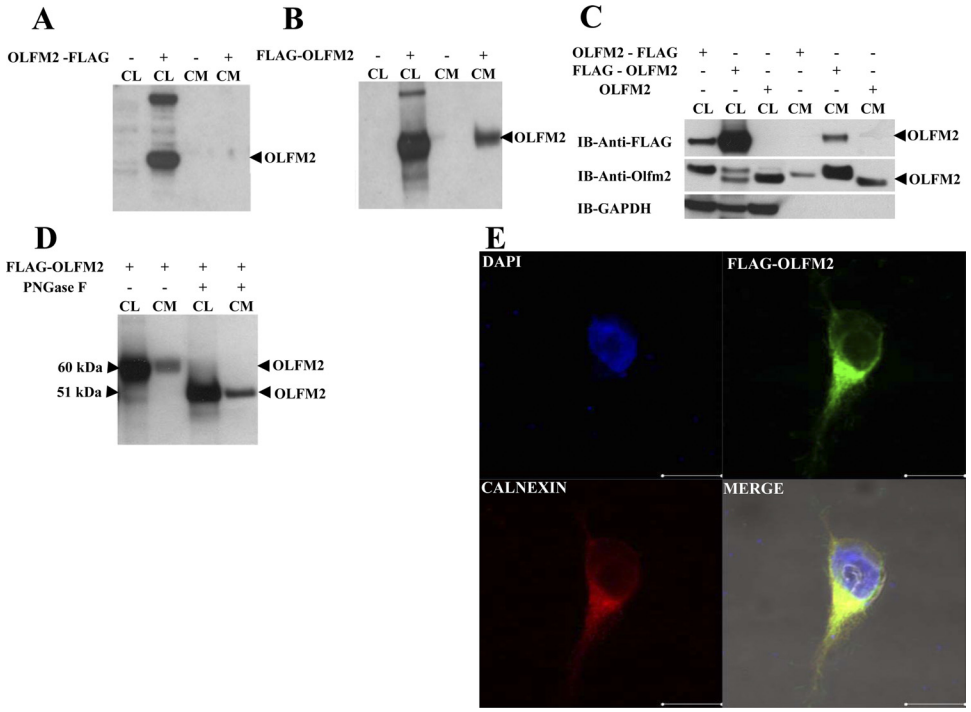

FIGURE 5. Secretion of OLFM2 protein from transfected HEK293 cells (**A**–**C**). The cells were transfected with the expression constructs encoding OLFM2 with the C-terminal (**A**) or the N-terminal FLAG (**B**) tag. The cells were transfected with the OLFM2-FLAG, FLAG-OLFM2, or OLFM2 expression constructs (**C**). CL and CM were analyzed by Western blot analysis with the indicated antibodies. The OLFM2 protein was represented by the upper band in the CL of the FLAG-OLFM2 construct (**C**). CL and CM from transfected HEK293 cells were treated with PNGase F (**D**). The size of a detected band after PNGase F treatment corresponded to the predicted molecular weight of OLFM2. (**E**). HEK293 cells were transfected with FLAG-OLFM2 plasmid. Immunofluorescence staining was performed with mouse monoclonal antibody against FLAG and rabbit polyclonal antibody against calnexin. Merged image shows the co-localization of FLAG-OLFM2 with endoplasmic reticulum marker. Nuclei were stained with DAPI. Scale bar, 5 μm.

sults of these experiments demonstrated that OLFM2 interacted well with Olfm1 and -3 (Figs. 6A–D) but did not interact with gliomedin ectodomain-His (Fig. 6F) and interacted only very weakly with myocilin in both cell lysates and CM (Fig. 6E). Similar to OLFM2, Olfm1 was also able to interact with Olfm3 (data not shown) confirming that these three proteins are able to form heterodimers.

OLFM2 Mutants May Prevent Secretion of Other Family Members

Two OLFM2 mutants, T86M and R144Q, have been reported to be associated with colorectal cancer[25] and glaucoma, respectively.[24] Both of these mutations are located outside the olfactomedin domain. It has been well demonstrated that glaucoma-causing mutations in myocilin prevent or reduce its secretion and that more than 90% of such mutations are located in the olfactomedin domain.[33–35] To test whether mutations in OLFM2 reduce its secretion, we produced two of the described mutants, T86M and R144Q. In addition, we produced the L420S mutation in the olfactomedin domain of OLFM2 corresponding to the severe glaucoma-causing I477S myocilin mutant. Although T86M and R144Q mutants were secreted similarly to wild-type OLFM2, secretion of the L420S mutant was completely blocked (Fig. 7A). We concluded that, similar to

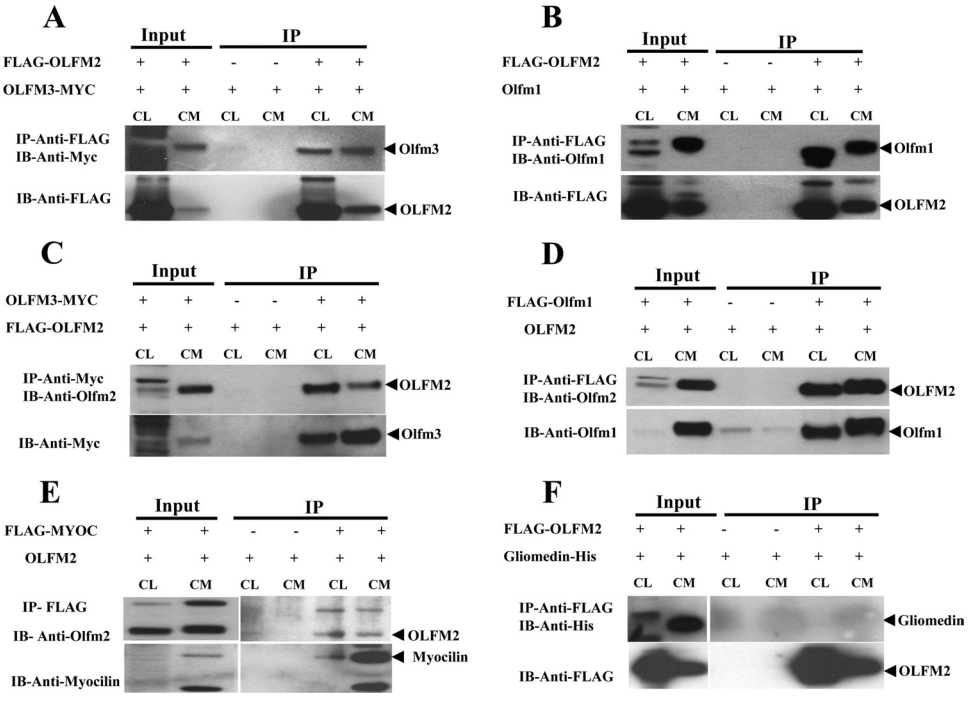

FIGURE 6. Interaction of OLFM2 with other family members. HEK293 cells were co-transfected with the indicated constructs. CM and CL were prepared 48 hours after transfection. Protein complexes were precipitated with FLAG antibody beads (**A**, **B**, **D**–**F**) or with Myc antibody (**C**). After immunoprecipitation (IP), proteins were eluted from the beads, separated by SDS-PAGE, and then probed with monoclonal antibodies against Myc (**A**), Olfm1 (**B**), Olfm2 (**C**–**E**), or His (**F**). Shown are Western blot analyses of CL and CM. These experiments were repeated at least two times. IB, immunoblots.

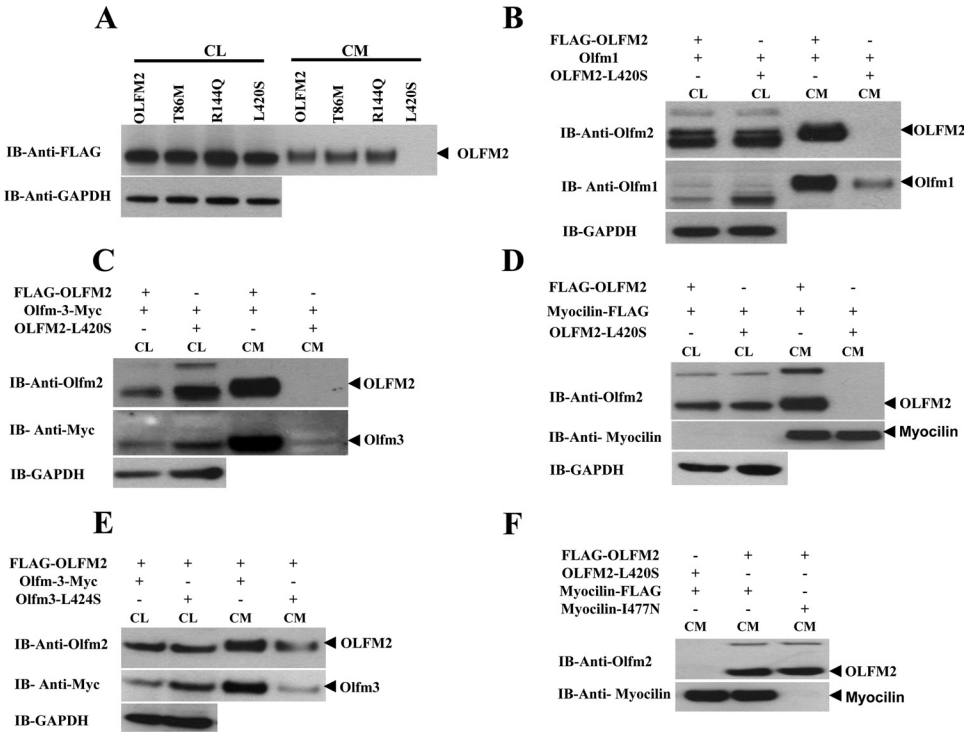

FIGURE 7. Effects of OLFM2 mutations on its secretion and interaction with other family members. HEK293 cells were co-transfected with the indicated constructs. CM and CL were prepared 48 hours after transfection. Shown are Western blot analysis of CM and CL probed with indicated antibodies. GAPDH staining was used for normalization of protein concentration in cell lysates. The mutation L420S in the olfactomedin domain inhibited the secretion of the OLFM2 protein (**A**). OLFM2–L420S mutation significantly inhibited the secretion of Olfm1 (**B**) and Olfm3 (**C**), whereas the secretion of myocilin was not affected (**D**). The secretion of OLFM2 was significantly inhibited by Olfm3–L424S mutation (**E**) whereas myocilin-I477N mutation did not affect the secretion of OLFM2 (**F**).

myocilin, some mutations in the olfactomedin domain of OLFM2 may block secretion of this protein. Moreover, co-transfection of the L420S OLFM2 mutant with wild-type Olfm1 or -3 significantly inhibited secretion of Olfm1 and -3 (Figs. 7B, 7C). However, when this mutant was co-transfected with wild-type myocilin, it did not inhibit secretion of myocilin (Fig. 7D). Similarly, the Olfm3 mutation L424S (the A form of Olfm3) corresponding to the I477S myocilin mutant not only blocked secretion of Olfm3 but also significantly inhibited secretion of wild-type OLFM2 (Fig. 7E). On the contrary, the I477N myocilin mutant was not secreted, but this did not affect secretion of wild-type OLFM2 (Fig. 7F). These results confirmed the interaction of OLFM2 with Olfm1 and -3 but not with myocilin and suggested that mutations in any of the three proteins, OLFM1, -2, and -3, may block secretion (and potentially activity) of the other two family members in vivo.

DISCUSSION

OLFM2 belongs to a highly conserved subfamily of olfactomedin domain–containing proteins. Human and mouse Olfm1, -2, and -3 show 98%, 96%, and 99% identity, respectively. High conservation of the OLFM2 sequence suggests that it might be essential for functioning of the tissues where it is expressed, but its function is still elusive.[9] Multiple N-terminal sequences encoded by different exons have been identified in human and mouse OLFM2. Most probably, different promoters are used to transcribe these forms in different tissues. The splice variant encoding 454-amino-acid OLFM2 is the most abundant variant in human neuronal tissues (ESTs database), and this variant was used in the current experiments. Olfm1 isoforms, with or without the olfactomedin domain, are produced as a result of alternative splicing in several species.[18,23] No isoforms without the olfactomedin domain were reported for OLFM2 or its closest homologue Olfm3.

Olfm2 is highly expressed in neuronal tissues during the course of embryonic development with maximum expression in the brain of newborn 6-day-old mice with subsequent down-regulation in adult brain. Analyses of transcriptome databases for astrocytes, neurons, and oligodendrocytes have demonstrated that *Olfm2* is expressed in oligodendrocyte precursors and is strongly downregulated in differentiated oligodendrocytes.[36] These data correspond to our observations, since the peak of gliogenesis in the mouse brain occurs between P5 and P20, and myelination occurs between P10 and P60.[37] Our data show that expression of *Olfm1* remains relatively stable after birth. In the eye, both *Olfm1* and *-2* are preferentially expressed in the developing retinal ganglion cells (Fig. 4). The peak of both *Olfm1* and *-2* expression is detected just before birth, and the level of expression is downregulated postnatally. This timetable of *Olfm1* and *-2* expression coincides with the completion of retinal ganglion cell differentiation. Published data suggest that *Olfm1* can be regarded as one of the markers of developing mouse retinal ganglion cells and is preferentially expressed in these cells between E12.5 and P0.[38] *Olfm1* is also expressed, to a lesser extent, in the adult retinal ganglion cells, and its expression in these cells is downregulated in a rat glaucoma model. In the developing zebrafish eye, *Olfm2* was detected, not only in the retinal ganglion cell layer but also in the inner nuclear layer.[31] Similarly, *Olfm3* which is most closely related to *Olfm2*, is expressed in both retinal ganglion and inner nuclear layers of adult rat retina.[19] It is interesting to note that another family member, *Olfm4*, is preferentially expressed in adult mouse Müller glial cells.[39] Available data suggest that Olfm1 may be involved in the regulation of retinal ganglion cell axon growth.[21] The functional roles of Olfm2, -3, and -4 in the retina are still not known.

Computer analysis of OLFM2 sequences indicates that Olfm2, similar to Olfm1 and -3, contains a signaling peptide and is a secreted protein. Perinuclear localization of OLFM2 in the endoplasmic reticulum of transfected cells (Fig. 5E) supports the idea that OLFM2 is a secreted protein. However, the efficiency of OLFM2 secretion is much lower than that of Olfm1 and -3. While the Olfm1 and -3, with C-terminal tags, were well secreted from transiently or stably transfected cells, similar OLFM2 constructs were not secreted. Only OLFM2 constructs

with a detection tag (FLAG) placed after the signaling peptide were moderately secreted. The Ser-Asp-Glu-Leu sequence was identified at the carboxyl terminus of *Xenopus* Olfm1 proteins (noelin-1 and noelin-2).[16] This sequence is similar but not identical with the consensus sequence Lys-Asp-Glu-Leu for protein retention in the endoplasmic reticulum. Blocking of this sequence by addition of Myc tag significantly improved secretion of *Xenopus* Olfm1.[16] Mammalian Olfm1 also contains the same Ser-Asp-Gln-Leu sequence at the C terminus but in our hands they were efficiently secreted from transfected cells (Fig. 6B). The Ser-Gly-Asp-Pro sequence is found at the carboxyl terminus of the human OLFM2 protein (Fig. 2) and this sequence should not serve as a retention signal. At present, we do not understand the observed differences in secretion of three closely related Olfm1-3 proteins. We also do not know how well OLFM2 is secreted from neuronal cells in vivo.

Several complete or partial knockouts of genes encoding olfactomedin domain-containing proteins have been produced, and none of them shows a strong phenotype. The list of these knockouts includes myocilin,[40] latrophilin 1,[41] gliomedin,[42] olfactomedin-like 3,[43] and Olfm1.[22] These data suggest that there are mechanisms to compensate for the effects of the elimination of these proteins.

Results of the present interaction study show that Olfm1, OLFM2, and Olfm3 proteins form heterodimers in the CLs and CM. The interaction of these proteins was further confirmed by the observation that mutations in one of the subfamily members that block its secretion significantly inhibited secretion of other subfamily members without mutations when co-expressed in the same cells. We tested the L420S OLFM2 mutant and the L424S Olfm3 mutant in our experiments. Although tested mutations in OLFM2 and Olfm3 have not been associated with any human abnormalities yet, we believe that mutations in the olfactomedin domain of Olfm1–3 proteins leading to human disease including eye disease will be identified in the future. Two reported OLFM2 mutants, T86M and R144Q, are associated with colorectal cancer[25] and glaucoma, respectively.[24] The disease with respect to mutations T86M and R144Q could be caused by altered cellular processes rather than accumulation of the protein due to reduced secretion. It is possible that these mutations in the *OLFM2* gene interact with changes in other genes to produce an observable disease. This effect is exemplified by a recent analysis of gene–gene interaction using common SNPs by Funayama et al.,[24] which indicated that OLFM2 and OPTN may interactively contribute to open-angle glaucoma.

An SNP associated with *Olfm2* has been recently identified in a scan for adaptive genetic divergence in West African cattle.[44] Although already-described variants do not reduce secretion of OLFM2 in the conditions that we used (Fig. 7), future studies may identify new OLFM2 variants which, similar to the L420S variant, strongly block protein secretion. Our data suggest that mutations in one of the closely related Olfm1-3 proteins that blocks its secretion may block secretion (and activity) of all subfamily members and may be more deleterious than knockout of a corresponding gene. At the same time, known glaucoma-causing mutations in the myocilin gene do not block secretion of the OLFM2 or Olfm1[45] proteins, and we believe that this is one of the reasons that these mutation do not lead to profound extraocular diseases.

Acknowledgments

The authors thank Heung Sun Kwon for myocilin constructs, Manuel Koch for the gliomedin ectodomain-His construct, and Thomas V. Johnson for critical reading of the manuscript.

References

1. Snyder DA, Rivers AM, Yokoe H, Menco BP, Anholt RR. Olfactomedin: purification, characterization, and localization of a novel olfactory glycoprotein. *Biochem.* 1991;30:9143–9153.
2. Karavanich CA, Anholt RR. Molecular evolution of olfactomedin. *Mol Biol Evolution.* 1998;15:718–726.
3. Hillier BJ, Vacquier VD. Amassin, an olfactomedin protein, mediates the massive intercellular adhesion of sea urchin coelomocytes. *J Cell Biol.* 2003;160:597–604.
4. Zeng LC, Han ZG, Ma WJ. Elucidation of subfamily segregation and intramolecular coevolution of the olfactomedin-like proteins by comprehensive phylogenetic analysis and gene expression pattern assessment. *FEBS Lett.* 2005;579:5443–5453.
5. Kulkarni NH, Karavanich CA, Atchley WR, Anholt RR. Characterization and differential expression of a human gene family of olfactomedin-related proteins. *Genet Res.* 2000;76:41–50.
6. Loria PM, Hodgkin J, Hobert O. A conserved postsynaptic transmembrane protein affecting neuromuscular signaling in Caenorhabditis elegans. *J Neurosci.* 2004;24:2191–2201.
7. Meyer E, Aglyamova GV, Wang S, et al. Sequencing and de novo analysis of a coral larval transcriptome using 454 GS-Flx. *BMC Genomics.* 2009;10:219.
8. Mukhopadhyay A, Talukdar S, Bhattacharjee A, Ray K. Bioinformatic approaches for identification and characterization of olfactomedin related genes with a potential role in pathogenesis of ocular disorders. *Mol Vis.* 2004;10:304–314.
9. Tomarev SI, Nakaya N. Olfactomedin s: possible mechanisms of action and functions in normal development and pathology. *Mol Neurobiol.* 2009;40:122–138.
10. Fingert JH, Heon E, Liebmann JM, et al. Analysis of myocilin mutations in 1703 glaucoma patients from five different populations. *Hum Mol Genet.* 1999;8:899–905.
11. Fingert JH, Stone EM, Sheffield VC, Alward WL. Myocilin glaucoma. *Surv Ophthalmol.* 2002;47:547–561.
12. Stone EM, Fingert JH, Alward WL, et al. Identification of a gene that causes primary open angle glaucoma. *Science.* 1997;275:668–670.
13. Kwon YH, Fingert JH, Kuehn MH, Alward WL. Primary open-angle glaucoma. *N Engl J Med.* 2009;360:1113–1124.
14. Adam MF, Belmouden A, Binisti P, et al. Recurrent mutations in a single exon encoding the evolutionarily conserved olfactomedin-homology domain of TIGR in familial open-angle glaucoma. *Hum Mol Genet.* 1997;6:2091–2097.
15. Barembaum M, Moreno TA, LaBonne C, Sechrist J, Bronner-Fraser M. Noelin-1 is a secreted glycoprotein involved in generation of the neural crest. *Nat Cell Biol.* 2000;2:219–225.
16. Moreno TA, Bronner-Fraser M. The secreted glycoprotein noelin-1 promotes neurogenesis in Xenopus. *Dev Biol.* 2001;240:340–360.
17. Nagano T, Nakamura A, Mori Y, et al. Differentially expressed olfactomedin-related glycoproteins (pancortins) in the brain. *Brain Res.* 1998;53:13–23.
18. Danielson PE, Forss-Petter S, Battenberg EL, deLecea L, Bloom FE, Sutcliffe JG. Four structurally distinct neuron-specific olfactomedin-related glycoproteins produced by differential promoter utilization and alternative mRNA splicing from a single gene. *J Neurosci Res.* 1994;38:468–478.
19. Torrado M, Trivedi R, Zinovieva R, Karavanova I, Tomarev SI. Optimedin: a novel olfactomedin-related protein that interacts with myocilin. *Hum Mol Genet.* 2002;11:1291–1301.
20. Moreno TA, Bronner-Fraser M. Noelins modulate the timing of neuronal differentiation during development. *Dev Biol.* 2005;288:434–447.
21. Nakaya N, Lee HS, Takada Y, Tzchori I, Tomarev SI. Zebrafish olfactomedin 1 regulates retinal axon elongation in vivo and is a modulator of Wnt signaling pathway. *J Neurosci.* 2008;28:7900–7910.
22. Cheng A, Arumugam TV, Liu D, et al. Pancortin-2 interacts with WAVE1 and Bcl-xL in a mitochondria-associated protein complex that mediates ischemic neuronal death. *J Neurosci.* 2007;27:1519–1528.
23. Nakaya N, Tomarev S. Expression patterns of alternative transcripts of the zebrafish olfactomedin 1 genes. *Gene Expr Patterns.* 2007;7:723–729.

24. Funayama T, Mashima Y, Ohtake Y, et al. SNPs and interaction analyses of noelin 2, myocilin, and optineurin genes in Japanese patients with open-angle glaucoma. *Invest Ophthalmol Vis Sci.* 2006;47:5368–5375.
25. Wood LD, Parsons DW, Jones S, et al. The genomic landscapes of human breast and colorectal cancers. *Science.* 2007;318:1108–1113.
26. Lee HS, Tomarev SI. Optimedin induces expression of N-cadherin and stimulates aggregation of NGF-stimulated PC12 cells. *Exp Cell Res.* 2007;313:98–108.
27. Thierry-Mieg D, Thierry-Mieg J. AceView: a comprehensive cDNA-supported gene and transcripts annotation. *Genome Biol.* 2006; 7(Suppl 1):S12.1–S12.14.
28. Senatorov V, Malyukova I, Fariss R, et al. Expression of mutated mouse myocilin induces open-angle glaucoma in transgenic mice. *J Neurosci.* 2006;26:11903–11914.
29. Maertens B, Hopkins D, Franzke CW, et al. Cleavage and oligomerization of gliomedin, a transmembrane collagen required for node of ranvier formation. *J Biol Chem.* 2007;282:10647–10659.
30. Kwon HS, Lee HS, Ji Y, Rubin JS, Tomarev SI. Myocilin is a modulator of Wnt signaling. *Mol Cell Biol.* 2009;29:2139–2154.
31. Lee JA, Anholt RR, Cole GJ. Olfactomedin-2 mediates development of the anterior central nervous system and head structures in zebrafish. *Mech Dev.* 2008;125:167–181.
32. Zielinska DF, Gnad F, Wisniewski JR, Mann M. Precision mapping of an in vivo N-glycoproteome reveals rigid topological and sequence constraints. *Cell.* 2010;141:897–907.
33. Gobeil S, Rodrigue MA, Moisan S, et al. Intracellular sequestration of hetero-oligomers formed by wild-type and glaucoma-causing myocilin mutants. *Invest Ophthalmol Vis Sci.* 2004;45:3560–3567.
34. Caballero M, Rowlette LL, Borras T. Altered secretion of a TIGR/MYOC mutant lacking the olfactomedin domain. *Biochim Biophys Acta.* 2000;1502:447–460.
35. Jacobson N, Andrews M, Shepard AR, et al. Non-secretion of mutant proteins of the glaucoma gene myocilin in cultured trabecular meshwork cells and in aqueous humor. *Hum Mol Genet.* 2001;10:117–125.
36. Cahoy JD, Emery B, Kaushal A, et al. A transcriptome database for astrocytes, neurons, and oligodendrocytes: a new resource for understanding brain development and function. *J Neurosci.* 2008; 28:264–278.
37. Baumann N, Pham-Dinh D. Biology of oligodendrocyte and myelin in the mammalian central nervous system. *Physiol Rev.* 2001;81: 871–927.
38. Trimarchi JM, Stadler MB, Roska B, et al. Molecular heterogeneity of developing retinal ganglion and amacrine cells revealed through single cell gene expression profiling. *J Comp Neurol.* 2007;502: 1047–1065.
39. Roesch K, Jadhav AP, Trimarchi JM, et al. The transcriptome of retinal Muller glial cells. *J Comp Neurol.* 2008;509:225–238.
40. Kim BS, Savinova OV, Reedy MV, et al. Targeted disruption of the myocilin gene (Myoc) suggests that human glaucoma-causing mutations are gain of function. *Mol Cell Biol.* 2001;21:7707–7713.
41. Tobaben S, Sudhof TC, Stahl B. Genetic analysis of alpha-latrotoxin receptors reveals functional interdependence of CIRL/latrophilin 1 and neurexin 1 alpha. *J Biol Chem.* 2002;277:6359–6365.
42. Feinberg K, Eshed-Eisenbach Y, Frechter S, et al. A glial signal consisting of gliomedin and NrCAM clusters axonal Na+ channels during the formation of nodes of Ranvier. *Neuron.* 2010;65:490–502.
43. Ikeya M, Kawada M, Nakazawa Y, et al. Gene disruption/knock-in analysis of mONT3: vector construction by employing both in vivo and in vitro recombinations. *Int J Dev Biol.* 2005;49:807–823.
44. Gautier M, Flori L, Riebler A, et al. A whole genome Bayesian scan for adaptive genetic divergence in West African cattle. *BMC Genomics.* 2009;10:550.
45. Malyukova I, Lee HS, Fariss RN, Tomarev SI. Mutated mouse and human myocilins have similar properties and do not block general secretory pathway. *Invest Ophthalmol Vis Sci.* 2006;47: 206–212.